Journal of Alloys and Compounds 509 (2011) 7139–7142

Contents lists available at ScienceDirect

Journal of Alloys and Compounds

journal homepage: www.elsevier.com/locate/jallcom

Growth and luminescence characteristics of Pr^{3+}-doped $Lu_{0.8}Sc_{0.2}BO_3$ single crystal

Yuntao Wu, Dongzhou Ding, Shangke Pan, Fan Yang, Guohao Ren*

Shanghai Institute of Ceramics, Chinese Academy of Sciences, No.215 Chengbei Road, Jiading, Shanghai 201800, PR China

ARTICLE INFO

Article history:
Received 11 February 2011
Received in revised form 5 April 2011
Accepted 5 April 2011
Available online 12 April 2011

Keywords:
Lutetium scandium orthoborate
Scintillation crystals
Praseodymium-doped
Luminescence characteristics

ABSTRACT

Transparent Pr^{3+}-doped $Lu_{0.8}Sc_{0.2}BO_3$ crystal has been grown by Czochralski method. The crystal structure is confirmed to be hexagonal with space group $R\bar{3}c$ checked by XRD measurement. The optical transmission spectra (absorption spectra), photoluminescence emission and excitation spectra, fluorescence decay time and the X-ray excited luminescence spectra of the crystal are measured at room temperature. The cut-off edge of this material locates at round 250 nm and there is a broad absorption in the region from 250–500 nm. The photoluminescence emission spectrum is dominated by fast $5d4f^1 \rightarrow 4f^2$ band peaking at 303 nm having 11.9 ns decay time. The measurement results show that the Pr^{3+}-doped $Lu_{0.8}Sc_{0.2}BO_3$ crystal, due to high density, fast decay time, high scintillation efficiency and non-hygroscopic property, could be a promising scintillator.

1. Introduction

Cerium activated lutetium orthoborate [1–4] is a promising scintillator with excellent characteristics. Although $LuBO_3:M^{3+}$ (M = Ce, Eu, Tb) materials have been recently made into scintillation films and composites [5–10], the high-temperature phase transformation [11,12] makes it hard to obtain bulk $LuBO_3$ single crystal directly from its melt. Nedelec et al. [13] once proposed that doping with rare earth ions can prevent the phase transformation in $LuBO_3$ to some extent, but the specific ions that can stabilize the calcite phase or vaterite phase were not confirmed. Recently, it was found that doping Sc^{3+} can stabilize the calcite phase of $LuBO_3$ and the $Lu_{0.9}Sc_{0.1}BO_3:Ce^{3+}$ crystals were proposed for applications in γ-ray detection [14,15]. In our earlier work [16], the influence of Sc/Lu ratio on phase transformation and luminescence properties of $Lu_{1-x}Sc_xBO_3$:Ce solid solutions have been investigated. Moreover, the Czochalski-grown $Lu_{0.8}Sc_{0.2}BO_3:Ce^{3+}$ crystal was found to be a promising material for scintillation application [17,18].

Compared to the Ce^{3+}-doped scintillators, Pr^{3+}-doped scintillators often have faster scintillation response due to its high energy shift by about 1.5 eV with respect to 5d–4f emission of Ce^{3+} [19]. This advantage makes the praseodymium-doped scintillators have always been the concern of researchers until now [20–22]. However, to our knowledge, there is no report about the luminescence characteristics of praseodymium doped lutetium scandium orthoborate crystal. In this paper, we report the preparation of Pr^{3+}-doped $Lu_{0.8}Sc_{0.2}BO_3$ crystal as well as its luminescence characteristics. Furthermore, the potential of Pr^{3+}-doped $Lu_{0.8}Sc_{0.2}BO_3$ crystal to be promising scintillator is also investigated.

2. Experimental

$Lu_{0.8}Sc_{0.2}BO_3$:0.5 at%Pr^{3+} single crystals were grown by the Czochralski method. Lu_2O_3, Sc_2O_3, Pr_6O_{11} and H_3BO_3 with purity of 4 N were used as raw materials and weighed in composition formula, except for H_3BO_3 which was 5 wt% rich due to vaporization loss during crystal growth. Mixtures of raw materials were calcined at 1200 °C for 20 h to initially complete the reaction and then charged in an iridium crucible of dimensions Ø60 × 40 mm^3. Crystals were grown in Argon atmosphere with 2 mm/h pulling rate and 10 rpm rotating rate. The dimensions of the ingots are round 30 mm in diameter and 10 mm in length. The $Lu_{0.8}Sc_{0.2}BO_3$:0.5 at%Pr^{3+} ingot, which was clear and no macroscopic imperfections, was cut into small samples of approximate dimensions 4 mm × 4 mm × 3 mm for all measurements and 4 mm × 4 mm × 1 mm only for optical transmission measurement. The commercial BGO single crystal with the size of 4 mm × 4 mm × 3 mm supplied by SICCAS was used as a reference to compare the relative light yield. The absolutely light yield of the BGO standard is 8500 ph/MeV.

The density of the $Lu_{0.8}Sc_{0.2}BO_3$:0.5 at%Pr^{3+} crystal was measured by the Archimedes method. The calculation equation is as follows:

$$\rho = \frac{m_0\rho_0}{(m_0 - m_1)} \quad (1)$$

where ρ is the density of the sample, m_0 is mass of the dried sample in air (unit: gram; need to dry the sample before testing), m_1 is the mass of fully immersed in water, ρ_0 is the density of distilled water at room temperature (1 g/cm^3). After calculation, the measured density of the $Lu_{0.8}Sc_{0.2}BO_3$:0.5 at%Pr^{3+} crystal is round 6.10 g/cm^3, quite similar to the density calculated according to its lattice parameters (6.15 g/cm^3).

Parts of grown crystals were crashed and ground into powders. The praseodymium concentration in crystal was measured by Varian ICP-AES instruments with 0.001 at% accuracy. The phases of these powders were characterized by Rigaku D\max-2550 V (scanning rate = 2.4°/min at 40 kV and 50 mA) where Cu Kα was used as incident X-ray (XRD measurement). Optical transmission spectrum (absorption spectrum), photoluminescence spectrum and fluorescence decay time

* Corresponding author. Tel.: +86 21 69987740; fax: +86 21 59927184.
E-mail addresses: caswyt@hotmail.com (Y. Wu), rgh@mail.sic.ac.cn (G. Ren).

0925-8388/$ – see front matter © 2011 Elsevier B.V. All rights reserved.
doi:10.1016/j.jallcom.2011.04.035

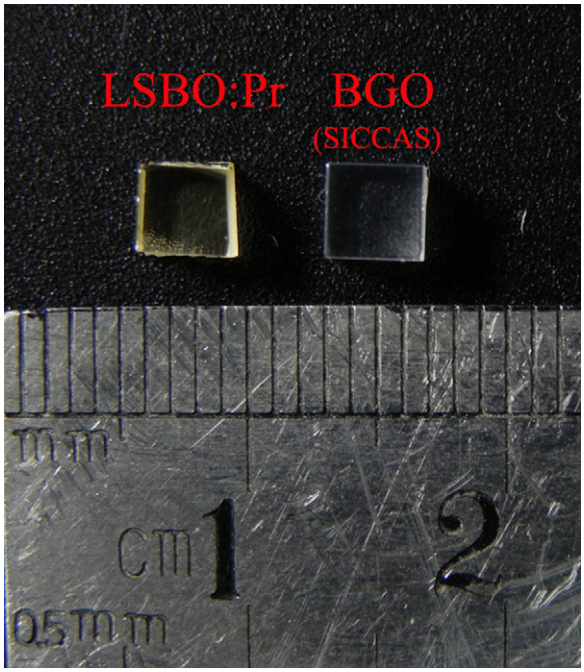

Fig. 1. Photos of double-polished $Lu_{0.8}Sc_{0.2}BO_3$:0.5 at%Pr^{3+} and BGO standard crystals.

curve were recorded on Perkin-Elmer Lambda 1050 UV/VIS/NIR spectrometer, the Perkin-Elmer LS50B and FLS-920 spectrofluorometer, respectively. The radioluminescence spectra excited by X-ray were recorded on an X-ray Excited Luminescence Spectrometer, assembled at Shanghai Institute of Ceramics.

3. Results and discussion

3.1. Crystal growth and crystal structure

Fig. 1 shows the photos of double-polished $Lu_{0.8}Sc_{0.2}BO_3$:0.5 at%Pr^{3+} and BGO standard crystals. The $Lu_{0.8}Sc_{0.2}BO_3$:0.5 at%Pr^{3+} crystal is transparent and in the color of pale-yellowed. The effective segregation coefficient can be calculated by the equation $k = C_s/C_0$, where C_s is the concentration of Pr ions in the grown crystal at the solidification fraction, C_0 is the initial concentration in the recipe, and k is the effective segregation coefficient. The concentration of Pr ions in the $Lu_{0.8}Sc_{0.2}BO_3$ crystal is 0.052 at%, measured by the ICP-AES. Therefore, the segregation coefficient of Pr ions is round 0.1, smaller than the value of Ce^{3+} in the same host [17]. The X-ray diffraction pattern of $Lu_{0.8}Sc_{0.2}BO_3$:0.5 at%Pr^{3+} is represented in Fig. 2. Compared to the PDF cards of $LuBO_3$ calcite phase and $ScBO_3$ calcite phase, the diffraction peaks of this sample can be well assigned to the calcite phase structure ($R\bar{3}c$ space system) with the characteristics of lutetium orthoborate ($LuBO_3$, PDF# 72-1053) and scandium orthoborate ($ScBO_3$, PDF# 79-0079) just with little differences in the diffraction angle. Therefore, the crystal structure is confirmed to be hexagonal with space group $R\bar{3}c$ and the sample is in the form of lutetium scandium orthoborate solid solution phase.

3.2. Optical characteristics

The optical transmission spectra from 200 to 800 nm of $Lu_{0.8}Sc_{0.2}BO_3$:0.5 at%Pr^{3+} crystals with different thickness are shown in Fig. 3. It is observed that the $Lu_{0.8}Sc_{0.2}BO_3$:0.5 at%Pr^{3+} crystals display one absorption band in the range from 210 to 250 nm. The similar absorption band can be also seen in $Lu_2Si_2O_7$:Pr^{3+} [20] and LuAG:Pr^{3+} crystals [21], which belongs to the $4f^2 \rightarrow 4f^15d$ transitions of Pr^{3+}. The dispersion of the on-set of

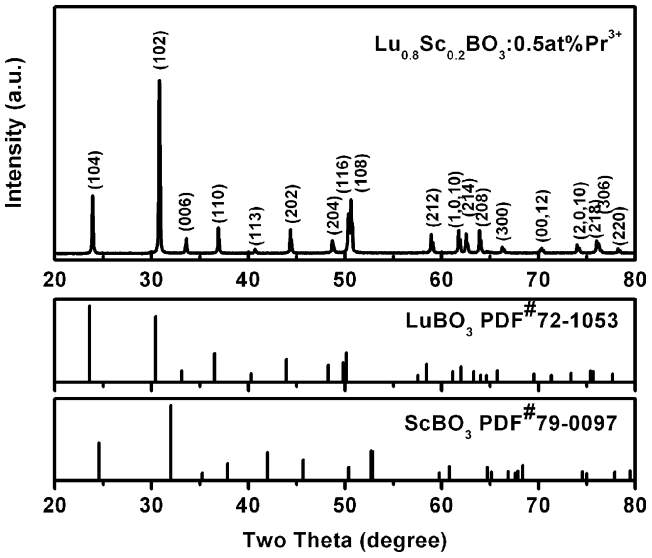

Fig. 2. X-ray diffraction patterns of $Lu_{0.8}Sc_{0.2}BO_3$:0.5 at%Pr^{3+} crystal powders (the PDF cards of $LuBO_3$ and $ScBO_3$ were used as references).

the cut-off edge locates at 250 nm, which has obviously blue-shift comparing to the value of LuAG:Pr^{3+} crystal round 300 nm [22] and similar with the value of $Lu_2Si_2O_7$:Pr^{3+} [23]. Although the maximum optical transmittance of $Lu_{0.8}Sc_{0.2}BO_3$:1 at%Pr^{3+} crystals with 1 mm and 3 mm thickness both can reach ~76%, there is an significant absorption valley locating in the region from 250 to 600 nm. The absorption intensity of this valley enhances with the increase of the sample thickness. We tentatively speculate that this absorption valley is related to intrinsic color of the crystal.

Fig. 4 shows the photoluminescence excitation (a) (λ_{em} = 303 nm), emission (b) (λ_{ex} = 234 nm) and absorption (c) spectra of $Lu_{0.8}Sc_{0.2}BO_3$:0.5 at%Pr^{3+} crystal at RT. In Fig. 4(a), the photoluminescence emission spectrum presents two types of emission bands: 4f → 4f emission bands between 500 and 710 nm corresponding to $^3P_J \rightarrow {}^3H_J$ transitions [24] and $5d^14f^1 \rightarrow 4f^2$ emission bands between 250 and 350 nm corresponding to the lowest crystal field component of the $4f^15d^1$ excited state to the $4f^2$ ground states: $^3H_4$, $^3H_5$, ($^3H_6$, $^3F_2$) and ($^3F_{3,4}$) levels (although could not be well resolved) [25]. The excitation bands at 218 nm and 234 nm (see Fig. 4(b)) within the not-well-resolved absorption bands (see Fig. 4(c)) are corresponding to the two lowest 4f($^3H_4$)

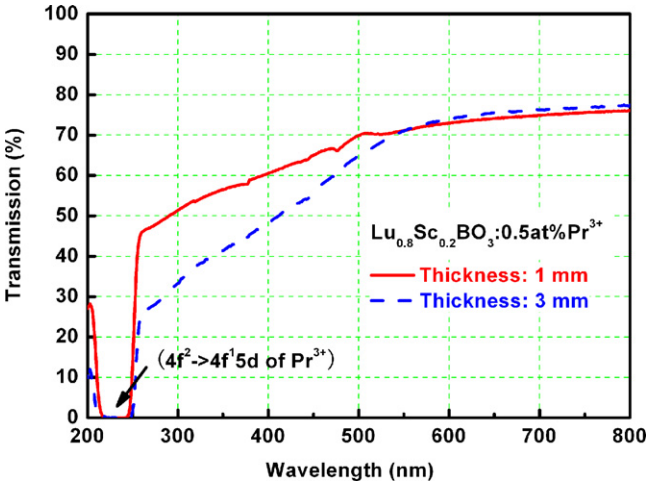

Fig. 3. Optical transmission curve of $Lu_{0.8}Sc_{0.7}BO_3$:0.5 at%Pr^{3+} crystal with different thickness.

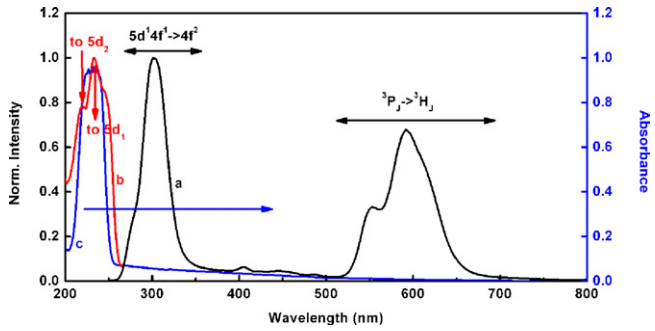

Fig. 4. Photoluminescence emission (a) (λ_{ex} = 234 nm), excitation (b) (λ_{em} = 303 nm) and absorption (c) spectra of $Lu_{0.8}Sc_{0.7}BO_3$:0.5 at%Pr^{3+} crystal at RT.

ground state to the $5d_{1,2}$ transitions of Pr^{3+}. Since the lowest $4f^15d^1$ excited state is located inside the band gap (about 180 nm) of $Lu_{0.8}Sc_{0.2}BO_3$ host (data not shown) and below the $4f^2\ {}^1S_0$ level (about 47,000 cm^{-1}), the fast and efficient $4f^15d^1 \rightarrow 4f^2$ luminescence could be expected if without the influence of luminescence quenching center (inefficient energy transfer).

The photoluminescence decay curves of $Lu_{0.8}Sc_{0.7}BO_3$:0.5 at%Pr^{3+} crystal are shown in Fig. 5. The emission decay at 303 nm and 600 nm under excitation at 234 nm are investigated, respectively. The solid curve of the sample can be well fitted with a single exponential decay $I(t) = I_0 \exp(-t/\tau)$, where I_0 is initial spectral intensity and τ is the decay time constant of the emission. The value of τ is found to be about 11.9 ns (χ^2 = 0.997) for Pr^{3+} $4f^15d^1 \rightarrow 4f^2$ emission (see Fig. 5(a)) and 11.8 ns (χ^2 = 0.997) for Pr^{3+} $^3P_J \rightarrow {}^3H_J$ emission (see Fig. 5(b)). It is well known that there are two principal procedures when a material is used as a scintillator, namely primary and secondary processes [26]. In the primary procedure the energy is transferred from the ionization state to the luminescent centers (Pr^{3+}), and the secondary procedure is that Pr^{3+} ion in the excited state returns to the ground state by combination luminescence. Though the decay time constant under 234 nm excitation in this paper belongs to the secondary processes, the value 11.9 ns ($4f^15d^1 \rightarrow 4f^2$ emission) is rather faster than the value 17.2 ns ($4f^15d^1 \rightarrow 4f^2$ emission) at RT of the secondary processes for LuAG:Pr^{3+} crystal [27]. Since the total decay time and the decay time constant of the primary procedure of a scintillator is quite important for practical application, the related measurements of $Lu_{0.8}Sc_{0.7}BO_3$:0.5 at%Pr^{3+} crystal are undergoing and the results will report in another paper.

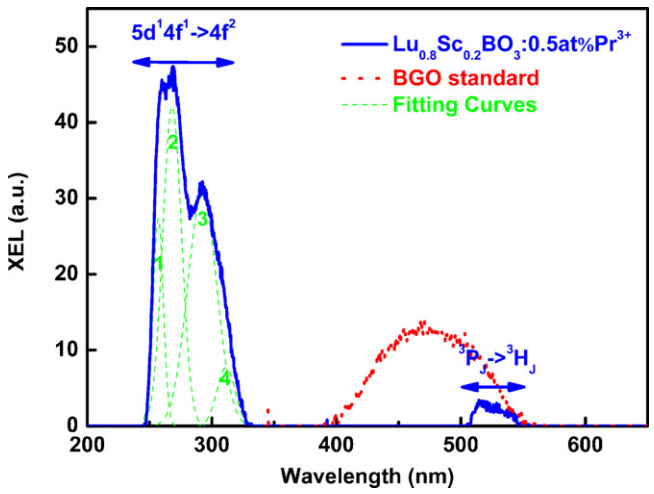

Fig. 6. X-ray excited luminescence spectra of $Lu_{0.8}Sc_{0.2}BO_3$:0.5 at%Pr^{3+} crystal (a) and BGO standard (b) at room temperature.

3.3. Scintillation properties

As a general rule, X-ray excited luminescence is supposed to determine the emission spectra of scintillation materials. The X-ray excited luminescence spectra of $Lu_{0.8}Sc_{0.2}BO_3$:0.5 at%Pr^{3+} crystal (a) and BGO standard (b) are presented in Fig. 6. Although the X-ray excited luminescence spectrum is composed of two types of emission bands similar with the PL spectrum, namely $4f \rightarrow 4f$ emission bands and $5d^14f^1 \rightarrow 4f^2$ emission bands, the relative intensity of two types of emission band in PL and XEL spectrum has significant difference. The $5d^14f^1 \rightarrow 4f^2$ emission bands are the main emission component in XEL spectrum, while the 4f–4f emission bands dominate in the PL spectrum. Unlike ultraviolet excitation, not only could the X-ray excitation directly stimulate the luminescence ion Pr3+, but also ionize the host and then transfer the energy to the energy levels of Pr3+ ion. Hence, we tentatively speculate that the cause of the above phenomenon results from the different energy distribution of the 5d and the 3PJ levels of Pr3+ for different excitation source. The $5d^14f^1 \rightarrow 4f^2$ emission bands in the region from 250 to 325 nm can be well resolved into four Gaussian components peaking at 256, 267, 290 and 309 nm, which are well agreement with the $5d^14f^1 \rightarrow 4f^2$ emission bands of Pr^{3+} in calcite phase $LuBO_3$ host [25].

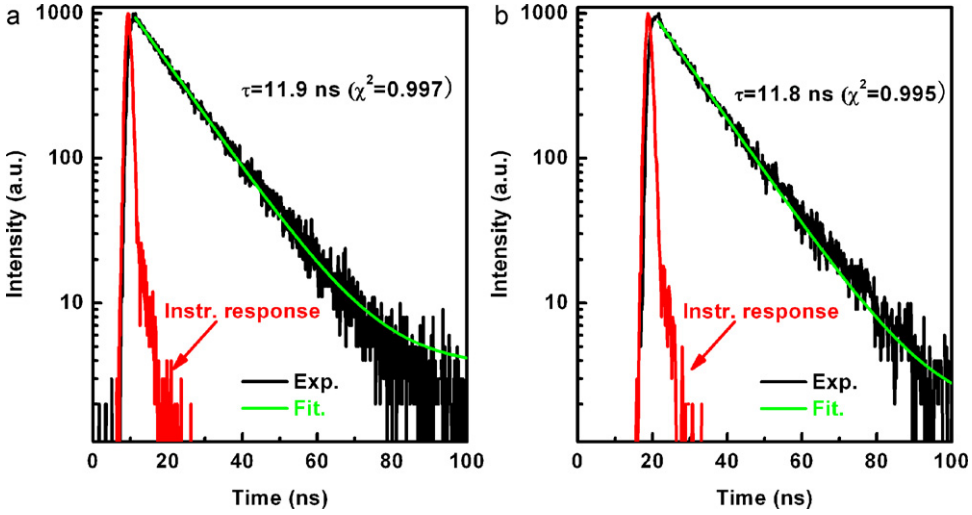

Fig. 5. Photoluminescence decay curves of the Pr^{3+} emission, (a) λ_{em} = 303 nm and λ_{ex} = 234 nm; (b) λ_{em} = 600 nm and λ_{ex} = 234 nm, RT.

Table 1
Characteristics of $Lu_{0.8}Sc_{0.2}BO_3$:0.5 at%Pr^{3+} and other typical scintillators.

Materials	Density (g/cm^3)	Scintillation efficiency (of BGO %)	Decay time (ns)	Emission wavelength (nm)	Hygroscopy	Ref.
NaI:Tl	3.67	470	230[a]	415	Strong	[29]
BGO	7.13	100	300[a]	480	No	[30]
LaBr:Ce^{3+}	5.29	718	35[a]	358	Strong	[29]
Lu_2SiO_5:Ce^{3+}	7.40	352	40[a]	420	No	[31]
$Lu_3Al_5O_{12}$:Pr^{3+}	6.67	300	20[a] (17.2[b])	308	No	[32,33]
$Lu_{0.8}Sc_{0.2}BO_3$:0.5 at%Pr^{3+}	6.10	~170	11.9[b]	256, 267, 290, 309	No	This work

The absolute light yield of BGO standard referred is 8500 ph/MeV.
[a] Represent that the decay time was obtained under c-ray excitation.
[b] Represent that the decay time was obtained under UV-excitation.

Based on the integral intensity calculated for XEL spectrum over 250–350 nm ($4f^15d^1 \rightarrow 4f^2$ emission bands of Pr^{3+}), it is estimated that the scintillation efficiency of $Lu_{0.8}Sc_{0.2}BO_3$:0.5 at%Pr^{3+} crystal corresponds to about 170% of the BGO standard scintillator (8500 ph/MeV), less than the value of LPS:Pr^{3+} (five times of BGO scintillator) [28]. The characteristics of $Lu_{0.8}Sc_{0.2}BO_3$:0.5 at%Pr^{3+} single crystal are shown in Table 1, together with the properties of some important commercial scintillators. Since the crystal quality and praseodymium concentration have not yet been optimized, higher light yield may be achieved. Hence, it is reasonable to believe that this crystal material is a good candidate for scintillation application especially as a medical imaging scintillator. The research on scintillation properties of $Lu_{0.8}Sc_{0.2}BO_3$:Pr^{3+} crystals is undergoing in our group.

4. Conclusion

Transparent $Lu_{0.8}Sc_{0.2}BO_3$:0.5 at%Pr^{3+} crystal with pale-yellowed color has been grown by Czochralski method. Its density is about 6.10 g/cm^3. Its crystal structure is confirmed to be hexagonal with space group $R\bar{3}c$. The segregation coefficient of Pr ions in $Lu_{0.8}Sc_{0.2}BO_3$ crystal is round 0.1. The cut-off edge of this material locates at round 250 nm and there is a broad absorption region from 250–500 nm, which possibly results from intrinsic color centers or micro defects. The emission spectrum is dominated by fast $5d4f^1 \rightarrow 4f^2$ band peaking at 303 nm having 11.9 ns decay time. The measurement results show that the Pr^{3+}-doped $Lu_{0.8}Sc_{0.2}BO_3$ crystal, due to high density (6.1 g/cm^3), fast decay time (11.9 ns), high scintillation efficiency (~170% BGO scintillator) and non-hygroscopic property, could be a promising scintillator by improving the crystal quality and praseodymium concentration.

Acknowledgment

This work was supported by the National Natural Science Foundation of China (grant no. 50902145), the Natural Science Foundation of Shanghai (grant no. 09ZR1435800), and the Knowledge Innovation Program of the Chinese Academy of Sciences (grant no. SCX200701). This document was prepared as an account of work sponsored by China.

References

[1] M.J. Weber, S.E. Derenzo, C. Dujardin, W.W. Moses, Proceedings of the International Conference on Inorganic Scintillators and Their Applications, September, 1995, pp. 325–328.
[2] W.W. Moses, M.J. Weber, S.E. Derenzo, D. Perry, P. Berdahl, Proceedings of the International Conference on Inorganic Scintillators and Their Applications, September, 1997, pp. 22–25.
[3] C.W.E. van Eijk, Proceedings of the International Conference on Inorganic Scintillators and their Applications, September, 1997, pp. 3–12.
[4] L. Zhang, C. Pedrini, C. Madej, C. Dujardin, J.C. Ga^^con, B. Moine, I. Kamenskikh, A. Belsky, D.A. Shaw, M.A. MacDonald, P. Mesnard, C. Fouassier, J.C. Van"t Spijker, C.E.W. Van Eijk, Radiat. Eff. Defects Solids 150 (1–4) (1999) 47–52.
[5] D. Boyer, F. Leroux, G. Bertrand, R. Mahiou, J. Non-Cryst. 306 (2002) 110–119.
[6] G. Chadeyron-Bertrand, D. Boyer, C. Dujardin, C. Mansuy, R. Mahiou, Nucl. Instrum. Methods Phys. Res. B 229 (2005) 232–239.
[7] C. Mansuy, E. Tomasell, R. Mahiou, L. Gengembre, J. Grimblot, J.M. Nedelec, Thin Solid Films 515 (2006) 666–669.
[8] C. Mansuy, J.M. Nedelec, R. Mahiou, J. Mater. Chem. 14 (2004) 3274–3280.
[9] J. Yang, C.X. Li, X.M. Zhang, Z.W. Quan, C.M. Zhang, H.Y. Li, J. Lin, Chem. Eur. J. 14 (2008) 4336–4345.
[10] C. Mansuy, J.M. Nedelec, C. Dujardin, R. Mahiou, J. Sol-Gel Sci. Technol. 32 (2004) 253–258.
[11] E. Levin, R.S. Roth, J.B. Martin, Am. Mineral. 46 (1961) 1030–1055.
[12] Y.T. Wu, D.Z. Ding, S.K. Pan, F. Yang, G.H. Ren, Phase Transitions (2010), doi:10.1080/01411594.2010.536887.
[13] J.-M. Nedelec, L. Courtheoux, E. Jallot, C. Kinowski, J. Lao, P. Laquerriere, C. Mansuy, G. Renaudin, S. Turrell, J. Sol-Gel Sci. Technol. 46 (2008) 259–271.
[14] S. Hatamoto, T. Yamazaki, J. Hasegawa, M. Katsurayam, M. Oshika, Y. Anzai, J. Cryst. Growth 311 (2009) 530–533.
[15] T. Yanagida, Y. Fujimoto, N. Kawaguchi, Y. Yokota, K. Kamada, D. Totsuka, S. Hatamoto, A. Yoshikawa, V. Chani, Nucl. Instrum. Methods. Phys. Res. A (2010), doi:10.1016/j.nima.2010.08.115.
[16] Y.T. Wu, D.Z. Ding, S.K. Pan, F. Yang, G.H. Ren, J. Alloys Compd. 509 (2011) 366–371.
[17] Y.T. Wu, D.Z. Ding, S.K. Pan, F. Yang, G.H. Ren, Cryst. Res. Technol. 46 (2011) 48–52.
[18] Y.T. Wu, D.Z. Ding, S.K. Pan, F. Yang, G.H. Ren, Opt. Mater. 33 (2011) 655–659.
[19] P. Dorenbos, J. Phys.: Condens. Matter 15 (2003) 8417–8434.
[20] J. Pejchal, M. Nikl, E. Mihóókováá, J.A. Mareš, A. Yoshikawa, H. Ogino, K.M. Schillemat, A. Krasnikov, A. Vedda, K. Nejezchleb, V. Múúččka, J. Phys. D: Appl. Phys. 42 (2009) 055117–055127.
[21] M. Nikl, H. Ogino, A. Yoshikawa, E. Mihokova, J. Pejchal, A. Beitlerova, A. Novoselov, T. Fukuda, Chem. Phys. Lett. 410 (2005) 218–221.
[22] T. Yanagida, A. Yoshikawa, A. Ikesue, K. Kamada, Y. Yokota, IEEE Trans. Nucl. Sci. 56 (2009) 2955–2959.
[23] H. Feng, G.H. Ren, Crystal growth and performance researches on the cerium doped rare-earth pyrosilicate $RE_2Si_2O_7$:Ce (RE=Lu, Gd, Y, Sc) scintillators, PhD thesis, Chinese Academy of Sciences, Shanghai, 2009, p. 90.
[24] L. Pidol, B. Viana, A. Kahn-Harari, A. Bessie're, P. Dorenbos, Nucl. Instrum. Methods Phys. Res. A 537 (2005) 125–129.
[25] L. Guerbous, O. Krachni, Radiat. Eff. Defects Solids 161 (2006) 199–206.
[26] H. Suzuki, T.A. Tombrello, C.L. Melcher, J.S. Schweitzer, IEEE Trans. Nucl. Sci. 41 (1994) 681–688.
[27] M. Nikl, H. Ogino, A. Krasnikov, A. Beitlerova, A. Yoshikawa, T. Fukuda, Phys. Status Solidi A 202 (2005) R4–R6.
[28] M. Nikl, G.H. Ren, D.Z. Ding, E. Mihokova, V. Jary, H. Feng, Chem. Phys. Lett. 493 (2010) 72–75.
[29] E.V.D. van Loef, P. Dorenbos, C.W.E. van Eijk, K. Kräämer, H.U. Güüdel, Appl. Phys. Lett. 79 (2001) 573–575.
[30] H. Suzuki, T.A. Tombrello, C.L. Melcher, J.S. Schweitzer, Nucl. Instrum. Methods A 320 (1992) 263–272.
[31] C.L. Melcher, J.S. Schweitzer, Nucl. Instrum. Methods A 314 (1992) 212–214.
[32] H. Ogino, A. Yoshikawa, M. Nikl, K. Kamada, T. Fukuda, J. Crystal Cryst. Growth 292 (2006) 239–242.
[33] M. Nikl, A. Yoshikawa, A. Vedda, T. Fukuda, J. Crystal Cryst. Growth 292 (2006) 416–421.